Structural Characterization of Five Sterically Protected Porphyrins

Carla Slebodnick, James C. Fettinger, Heidi B. Peterson, and James A. Ibers*

Contribution from the Department of Chemistry, Northwestern University, Evanston, Illinois 60208-3113

Received November 1, 1995[⊗]

Abstract: The structures of the sterically protected "pocket" porphyrin H_2(α-PocPivP) (**1**), and the "capped" porphyrins H_2(C_3-Cap) (**2**), Fe(C_3-Cap)(CO)(1-MeIm) (**3**), H_2(C_4-Cap) (**4**), and Fe(C_4-Cap)(Cl) (**5**) have been determined by single-crystal X-ray diffraction methods. Compounds **1-4** each pack with one independent porphyrin unit and solvate molecules in the unit cell. Compound **5** packs with two crystallographically independent porphyrins and solvate molecules in the unit cell. The structure of **1** is the first of a pocket porphyrin in which there are no ligands bound inside the protected region. This structure reveals that the main form of distortion that occurs when a ligand binds inside the protected region is the lateral movement of the benzene cap relative to a position above the centroid of the porphyrin. In **1** this lateral displacement is 1.86 Å whereas this displacement is 3.30 Å in Fe(*β*-PocPivP)(CO)(1,2-Me_2Im). Comparison of the free-base structure **2** with the Fe^{II} carbonyl **3**, where the CO ligand is bound under the cap and the 1-MeIm ligand is bound opposite the cap, reveals that there is little lateral distortion in the C_3-Cap system, but there is significant vertical expansion of the cap upon coligation to the Fe center. The distance of the cap centroid from the mean porphyrin plane increases 2.37 Å to accommodate the CO ligand, from 3.49 Å in **2** to 5.86 Å in **3**. The Fe−C−O angle in **3** is 178.0(13)°. In the structures of the C_4-Cap system **4** and **5** there is sufficient space for the binding of small ligands, such as CO and O_2, as well as larger ligands. Compound **4** crystallizes with a $CHCl_3$ solvate molecule under the cap. The distances from cap centroid to porphyrin plane in the C_4-Cap structures are 7.28, 7.12, and 7.66 Å for **4**, **5A**, and **5B**, respectively. This is significantly greater than the distance of 5.6 Å in Fe(C_2-Cap)(CO)(1-MeIm) and 5.86 Å in **3**. The relation between these structural changes on ligation and the binding properties of these systems for CO and O_2 is explored.

Introduction

The study of the binding of small molecules to sterically protected porphyrins that model the heme active site, along with structural characterization of these systems, has been an active method of probing important structure−function relationships exhibited by the hemoproteins hemoglobin (Hb) and myoglobin (Mb).[1−4] One relationship of Hb and Mb for which model compounds have been especially useful is their discrimination against the binding of CO.[4] Compared with nonbiological porphyrins, the value of $M = P_{1/2}{}^{O_2}/P_{1/2}{}^{CO}$ [5] for Hb and Mb is significantly smaller, and hence either O_2 binding is stabilized in biological systems or CO binding is destabilized. In fact it is likely that both of these processes contribute to the lower value of *M*. However, the chemistry of the two processes is different, and the processes can be addressed separately through the proper design of model systems. The argument for the stabilization of O_2 binding rests on the electronic environment about the O_2 ligand whereas the argument for destabilization against CO binding assumes that steric forces are exerted on the CO ligand.[6] A more polar environment inside the protein cavity, including hydrogen bonding, is tailored to stabilize the polar Fe−O_2 bond while having little effect on the relatively nonpolar Fe−CO bond. Destabilization of CO binding is believed to be the result of a steric barrier created by the protein. This barrier makes the binding of CO, which prefers a linear conformation,[7] energetically unfavorable while still allowing enough space for O_2, which prefers a bent geometry.[8] Protein structure determinations have provided a wide range of Fe−C−O angles,[9−12] but lack of precision in such determinations weakens support for steric constraints on the bound CO ligand.

To address the nature of steric discrimination against the binding of CO many types of sterically encumbered porphyrins have been synthesized over the past quarter century. Representative examples include "strapped",[13−19] "picnic basket",[20−24]

[⊗] Abstract published in *Advance ACS Abstracts,* March 15, 1996.

(1) David, S.; Dolphin, D.; James, B. R. In *Frontiers in Bioinorganic Chemistry*; Xavier, A. V., Ed.; VCH: Weinheim, 1986; pp 163−182.

(2) Jameson, G. B.; Ibers, J. A. *Comments Inorg. Chem.* **1983**, *2*, 97−126.

(3) Momenteau, M.; Reed, C. A. *Chem. Rev.* **1994**, *94*, 659−698.

(4) Jameson, G. B.; Ibers, J. A. In *Bioinorganic Chemistry*; Bertini, I., Gray, H. B., Lippard, S. J., Valentine, J. S., Eds.; University Science Books: Mill Valley, CA, 1994; pp 167−252.

(5) $M = P_{1/2}{}^{O_2}/P_{1/2}{}^{CO}$, where $P_{1/2}{}^{L}$ is the partial pressure of L (L = CO, O_2) at half saturation.

(6) Collman, J. P.; Brauman, J. I.; Halbert, T. R.; Suslick, K. S. *Proc. Natl. Acad. Sci. U.S.A.* **1976**, *73*, 3333−3337.

(7) Peng, S.-M.; Ibers, J. A. *J. Am. Chem. Soc.* **1976**, *98*, 8032−8036.

(8) Jameson, G. B.; Rodley, G. A.; Robinson, W. T.; Gagne, R. R.; Reed, C. A.; Collman, J. P. *Inorg. Chem.* **1978**, *17*, 850−857.

(9) Quillin, M. L.; Arduini, R. M.; Olson, J. S.; Phillips, G. N., Jr. *J. Mol. Biol.* **1993**, *234*, 140−155.

(10) Cheng, X.; Schoenborn, B. P. *J. Mol. Biol.* **1991**, *220*, 381−399.

(11) Derewenda, Z.; Dodson, G.; Emsley, P.; Harris, D.; Nagai, K.; Perutz, M.; Reynaud, J.-P. *J. Mol. Biol.* **1990**, *211*, 515−519.

(12) Kuriyan, J.; Wilz, S.; Karplus, M.; Petsko, G. A. *J. Mol. Biol.* **1986**, *192*, 133−154.

(13) Baldwin, J. E.; Crossley, M. J.; Klose, T.; O'Rear, E. A., III; Peters, M. K. *Tetrahedron* **1982**, *38*, 27−39.

(14) Ricard, L.; Fischer, J.; Weiss, R.; Momenteau, M. *Nouv. J. Chim.* **1984**, *8*, 639−642.

(15) Traylor, T. G.; Mitchell, M. J.; Tsuchiya, S.; Campbell, D. H.; Stynes, D. V.; Koga, N. *J. Am. Chem. Soc.* **1981**, *103*, 5234−5236.

(16) Traylor, T. G.; Tsuchiya, S.; Campbell, D.; Mitchell, M.; Stynes, D.; Koga, N. *J. Am. Chem. Soc.* **1985**, *107*, 604−614.

(17) David, S.; James, B. R.; Dolphin, D.; Traylor, T. G.; Lopez, M. A. *J. Am. Chem. Soc.* **1994**, *116*, 6−14.

(18) David, S.; Dolphin, D.; James, B. R.; Paine, J. B., III; Wijesekera, T. P.; Einstein, F. W. B.; Jones, T. *Can. J. Chem.* **1986**, *64*, 208−212.

(19) Traylor, T. G.; Koga, N.; Deardurff, L. A.; Swepston, P. N.; Ibers, J. A. *J. Am. Chem. Soc.* **1984**, *106*, 5132−5143.

(20) Collman, J. P.; Brauman, J. I.; Fitzgerald, J. P.; Hampton, P. D.; Naruta, Y.; Sparapany, J. W.; Ibers, J. A. *J. Am. Chem. Soc.* **1988**, *110*, 3477−3486.

0002-7863/96/1518-3216$12.00/0

"picket fence",[25−28] "pocket",[28−30] and "capped" [31−38] porphyrins as well as hybrids of these different classifications.[39,40] The binding of CO and O_2 to these model systems has been studied extensively. However, owing to the difficulty of obtaining crystals of these elaborated porphyrin systems, especially those where O_2 is a ligand, only limited structural data are available. Here we report the structural characterization of the pocket porphyrin H_2(α-PocPivP)[29,30,41] and the capped porphyrins H_2(C_3-Cap),[31,41] Fe(C_3-Cap)(CO)(1-MeIm),[33] H_2(C_4-Cap),[41] and Fe(C_4-Cap)(Cl).[34] The pocket porphyrin structure will be compared with the structures of Fe(*β*-PocPivP)(CO)(1-MeIm),[42] Ru(α-PocPivP)(CO)(1-MeIm),[43] and Ru(*β*-PocPivP)$(H_2O)_{in}$-$(CO)_{out}$.[44] The capped porphyrin structures will be compared with those known for the C_2-Cap system, namely H_2(C_2-Cap),[45] Fe(C_2-Cap)(CO)(1-MeIm),[46] and Fe(C_2-Cap)(Cl),[47] and the C_3-Cap structure will be compared with that of Co(C_3-Cap).[48] Close examination of the structural changes that take place when small molecules bind under the cap will be used to address the binding behavior previously reported for these pocket[28] and capped porphyrin[32−34,49,50] systems.

Experimental Section

Material. All solvents were reagent grade. Methanol was dried by refluxing over $Mg(OCH_3)_2$; $CHCl_3$ was dried by refluxing over CaH_2. C_6F_6 was stored over 4 Å molecular sieves and *n*-hexane was refluxed over Na. $Na_2S_2O_4$ was purchased from Aldrich and used without further purification. H_2(α-PocPivP)[29] was a gift from Prof. J. P. Collman. H_2-(C_3-Cap), Fe(C_3-Cap)(Cl), H_2(C_4-Cap), and Fe(C_4-Cap)(Cl) were kindly supplied by Prof. J. E. Baldwin.[31]

X-ray Structure Determinations. Data were collected on either an Enraf Nonius CAD4 or a Picker diffractometer. Unit cell parameters were determined by least-squares refinement of at least 25 reflections that had been automatically centered on the diffractometer. Intensity data were collected, processed by methods standard in the laboratory for the individual diffractometers, and corrected for absorption.[51] The direct methods program SHELXS[52] was used for structure solution and the program SHELXL-93[53] for structure refinement. The program package SHELXTL PC[52] was used for the ensuing molecular graphics generation.

H_2(α-PocPivP)·2.5C_6F_6. H_2(α-PocPivP) (**1**) (∼4 mg) was dissolved in a 1:4 solution of $CHCl_3$ and C_6F_6 (∼8 mL), and the solvents were allowed to evaporate slowly over a period of several months. X-ray quality crystals formed just above the solvent level. The trapezoid shaped crystals were too large, and the chosen crystal was cut into a block.

This purple block was coated with Krytox oil[54] to prevent solvent evaporation. It was then mounted in the cold stream of an Enraf Nonius CAD4 diffractometer. Cell reduction and systematic absences were consistent with the monoclinic space group C_{2h}^5-$P2_1/n$. Crystallographic details are given in Table 1. The final refinement[53] on F^2 involved an anisotropic model for all non-hydrogen atoms and fixed positions for the hydrogen atoms. There were 12 879 independent observations and 931 variables. This refinement converged to the *R* indices given in Table 1. The atom-labeling scheme is given in Figure 1. Table 2 provides selected bond distances. Additional crystallographic data, atomic coordinates and equivalent isotropic displacement parameters, additional bond lengths and angles, anisotropic displacement parameters, and hydrogen-atom coordinates and isotropic displacement parameters are available in Tables SI−SV.[55]

H_2(C_3-Cap)·$CHCl_3$·3C_6H_{14}. H_2(C_3-Cap) (**2**) was dissolved in $CHCl_3$. *n*-Hexane was allowed to diffuse into the solution over a period

(21) Ricard, L.; Weiss, R.; Momenteau, M. *J. Chem. Soc., Chem. Commun*. **1986**, 818−820.
(22) Schappacher, M.; Fisher, J.; Weiss, R. *Inorg. Chem*. **1989**, *28*, 389−390.
(23) Collman, J. P.; Brauman, J. I.; Fitzgerald, J. P.; Sparapany, J. W.; Ibers, J. A. *J. Am. Chem. Soc*. **1988**, *110*, 3486−3495.
(24) Collman, J. P.; Zhang, X.; Wong, K.; Brauman, J. I. *J. Am. Chem. Soc*. **1994**, *116*, 6245−6251.
(25) Collman, J. P.; Gagne, R. R.; Reed, C. A.; Halbert, T. R.; Lang, G.; Robinson, W. T. *J. Am. Chem. Soc*. **1975**, *97*, 1427−1439.
(26) Collman, J. P.; Brauman, J. I.; Doxsee, K. M.; Halbert, T. R.; Suslick, K. S. *Proc. Natl. Acad. Sci. U.S.A*. **1978**, *75*, 564−568.
(27) Wuenschell, G. E.; Tetreau, C.; Lavalette, D.; Reed, C. A. *J. Am. Chem. Soc*. **1992**, *114*, 3346−3355.
(28) Collman, J. P.; Brauman, J. I.; Iverson, B. L.; Sessler, J. L.; Morris, R. M.; Gibson, Q. H. *J. Am. Chem. Soc*. **1983**, *105*, 3052−3064.
(29) Collman, J. P.; Brauman, J. I.; Collins, T. J.; Iverson, B. L.; Lang, G.; Pettman, R. B.; Sessler, J. L.; Walters, M. A. *J. Am. Chem. Soc*. **1983**, *105*, 3038−3052.
(30) Collman, J. P.; Brauman, J. I.; Collins, T. J.; Iverson, B.; Sessler, J. L. *J. Am. Chem. Soc*. **1981**, *103*, 2450−2452.
(31) Almog, J.; Baldwin, J. E.; Crossley, M. J.; Debernardis, J. F.; Dyer, R. L.; Huff, J. R.; Peters, M. K. *Tetrahedron* **1981**, *37*, 3589−3601.
(32) Budge, J. R.; Ellis, P. E., Jr.; Jones, R. D.; Linard, J. E.; Szymanski, T.; Basolo, F.; Baldwin, J. E.; Dyer, R. L. *J. Am. Chem. Soc*. **1979**, *101*, 4762−4763.
(33) Hashimoto, T.; Dyer, R. L.; Crossley, M. J.; Baldwin, J. E.; Basolo, F. *J. Am. Chem. Soc*. **1982**, *104*, 2101−2109.
(34) Shimizu, M.; Basolo, F.; Vallejo, M. N.; Baldwin, J. E. *Inorg. Chim. Acta* **1984**, *91*, 247−250.
(35) Garcia, B.; Lee, C.-H.; Blaskó, A.; Bruice, T. C. *J. Am. Chem. Soc*. **1991**, *113*, 8118−8126.
(36) Zhang, H.-Y.; Blaskó, A.; Yu, J.-Q.; Bruice, T. C. *J. Am. Chem. Soc*. **1992**, *114*, 6621−6630.
(37) Johnson, M. R.; Seok, W. K.; Ibers, J. A. *J. Am. Chem. Soc*. **1991**, *113*, 3998−4000.
(38) Collman, J. P.; Zhang, X.; Herrmann, P. C.; Uffelman, E. S.; Boitrel, B.; Straumanis, A.; Brauman, J. I. *J. Am. Chem. Soc*. **1994**, *116*, 2681−2682.
(39) Baldwin, J. E.; Cameron, J. H.; Crossley, M. J.; Dagley, I. J.; Hall, S. R.; Klose, T. *J. Chem. Soc., Dalton Trans*. **1984**, 1739−1746.
(40) Tetreau, C.; Lavalette, D.; Momenteau, M.; Fischer, J.; Weiss, R. *J. Am. Chem. Soc*. **1994**, *116*, 11840−11848.
(41) Abbreviations: PocPivP = a porphyrin with three $-CH_2(CO)NH-$ linkages connecting the 1,3,5-positions of a benzene cap to the ortho positions of TPP and a pivalamido arm extending from the ortho position of the fourth phenyl group of TPP in either the α (toward the cap) or *β* (away from the cap) direction; TPP = tetraphenylporphyrinato dianion; C_n-Cap = a capped porphyrin with four $-(CO)O(CH_2)_nO-$ linkages connecting the 1,2,4,5-positions of a benzene cap to the ortho positions of TPP; 1-MeIm = 1-methylimidazole; 1,2-Me_2Im = 1,2-dimethylimidazole; Py = pyridine; 1,5-DCIm = 1,5-dicyclohexylimidazole; Deut = deuteroporphyrinato dianion; Proto = protoporphyrin IX dimethyl ester dianion; TTOMePP = *meso*-tetra(3,4,5-trimethoxyphenyl)porphyrinato dianion; Piv_2C_n ($n = 6-10$) = porphyrin with a strap of the type $-NH(CO)(CH_2)_n(CO)NH-$ linking the ortho positions of opposite phenyl groups of TPP and pivalamido groups extending from the ortho positions of the remaining two phenyl groups of TPP in the α direction; $Ph_{5,5}$-BHP = porphyrin with two straps of the type $-O(CH_2)_4-$ linking the 1,4 positions of a benzene cap to opposite phenyl groups of TPP, one strap on each face of the porphyrin; Durene-*n*/*n* = a strapped porphyrin with a 1,4-substituted, 2,3,5,6-tetramethylbenzene cap containing $-(CH_2)_n-$ chains bonded to the trans pyrrole rings of a porphyrin that is alkylated with methyl or ethyl groups at the other *β*-pyrrolic positions.
(42) Kim, K.; Fettinger, J.; Sessler, J. L.; Cyr, M.; Hugdahl, J.; Collman, J. P.; Ibers, J. A. *J. Am. Chem. Soc*. **1989**, *111*, 403−405.
(43) Slebodnick, C.; Seok, W. K.; Kim, K.; Ibers, J. A. *Inorg. Chim. Acta*, in press.
(44) Slebodnick, C.; Kim, K.; Ibers, J. A. *Inorg. Chem*. **1993**, *32*, 5338−5342.
(45) Jameson, G. B.; Ibers, J. A. *J. Am. Chem. Soc*. **1980**, *102*, 2823−2831.
(46) Kim, K.; Ibers, J. A. *J. Am. Chem. Soc*. **1991**, *113*, 6077−6081.
(47) Sabat, M.; Ibers, J. A. *J. Am. Chem. Soc*. **1982**, *104*, 3715−3721.
(48) Sparapany, J. W.; Crossley, M. J.; Baldwin, J. E.; Ibers, J. A. *J. Am. Chem. Soc*. **1988**, *110*, 4559−4564.
(49) Linard, J. E.; Ellis, P. E., Jr.; Budge, J. R.; Jones, R. D.; Basolo, F. *J. Am. Chem. Soc*. **1980**, *102*, 1896−1904.
(50) Rose, E. J.; Venkatasubramanian, P. N.; Swartz, J. C.; Jones, R. D.; Basolo, F.; Hoffman, B. M. *Proc. Natl. Acad. Sci. U.S.A*. **1982**, *79*, 5742−5745.
(51) de Meulenaer, J.; Tompa, H. *Acta Crystallogr*. **1965**, *19*, 1014−1018.
(52) Sheldrick, G. M. SHELXTL PC Version 5.0 An Integrated System for Solving, Refining, and Displaying Crystal Structures from Diffraction Data. Siemens Analytical X-Ray Instruments, Inc. Madison, WI, 1994.
(53) Sheldrick, G. M. *J. Appl. Crystallogr*., to be submitted.
(54) Krytox oil is a product of Dupont.
(55) Supporting information.

Table 1. Selected Crystallographic Data

compd	H_2(α-PocPivP) (**1**)	H_2(C_3-Cap) (**2**)	Fe(C_3-Cap)(CO)(1-MeIm) (**3**)	H_2(C_4-Cap) (**4**)	Fe(C_4-Cap)(Cl) (**5**)
chem formula	$C_{61}H_{46}N_8O_4{\cdot}2.5C_6F_6$	$C_{66}H_{52}N_4O_{12}{\cdot}CHCl_3{\cdot}3C_6H_{14}$	$C_{71}H_{52}FeN_6O_{13}{\cdot}CHCl_3{\cdot}2H_2O$	$C_{70}H_{56}N_4O_{12}{\cdot}2CHCl_3$	$C_{70}H_{60}ClFeN_4O_{12}{\cdot}1/2CHCl_3{\cdot}1/2C_6H_{14}$
fw	1420	1471	1408	1384	1318
space group	C_{2h}^5-$P2_1/n$	C_{2h}^5-$P2_1/n$	C_{2h}^5-$P2_1/c$	D_{2h}^{14}-$Pbca$	C_i^1-$P\bar{1}$
a, Å	16.920(2)	20.546(8)	18.422(12)	14.359(3)	17.841(6)
b, Å	21.565(2)	15.661(7)	15.932(12)	20.803(4)	18.125(4)
c, Å	17.989(1)	22.919(9)	22.54(2)	43.690(9)	24.953(9)
α, deg	90	90	90	90	111.83(3)
β, deg	97.664(8)	111.144(12)	90.76(2)	90	98.85(3)
γ, deg	90	90	90	90	93.79(2)
V, Å^3	6505(1)	6878(5)	6614(8)	13051(5)	7334(4)
Z	4	4	4	8	4
density, g/cm^3	1.450	1.420	1.414	1.409	1.194
radiation (*λ*, Å)	Cu Kα (1.5406)	Cu Kα (1.5406)	Mo Kα$_1$ (0.7093)	Mo Kα$_1$ (0.7093)	Cu Kα (1.5406)
μ, cm^{-1}	10	18	4	3	30
T, °C	−167(2)	−167(2)	−167(2)	−167(2)	−167(2)
R(*F*)	0.074	0.12	0.15	0.17	0.15
$R_w(F^2)$	0.206	0.254	0.297	0.310	0.264

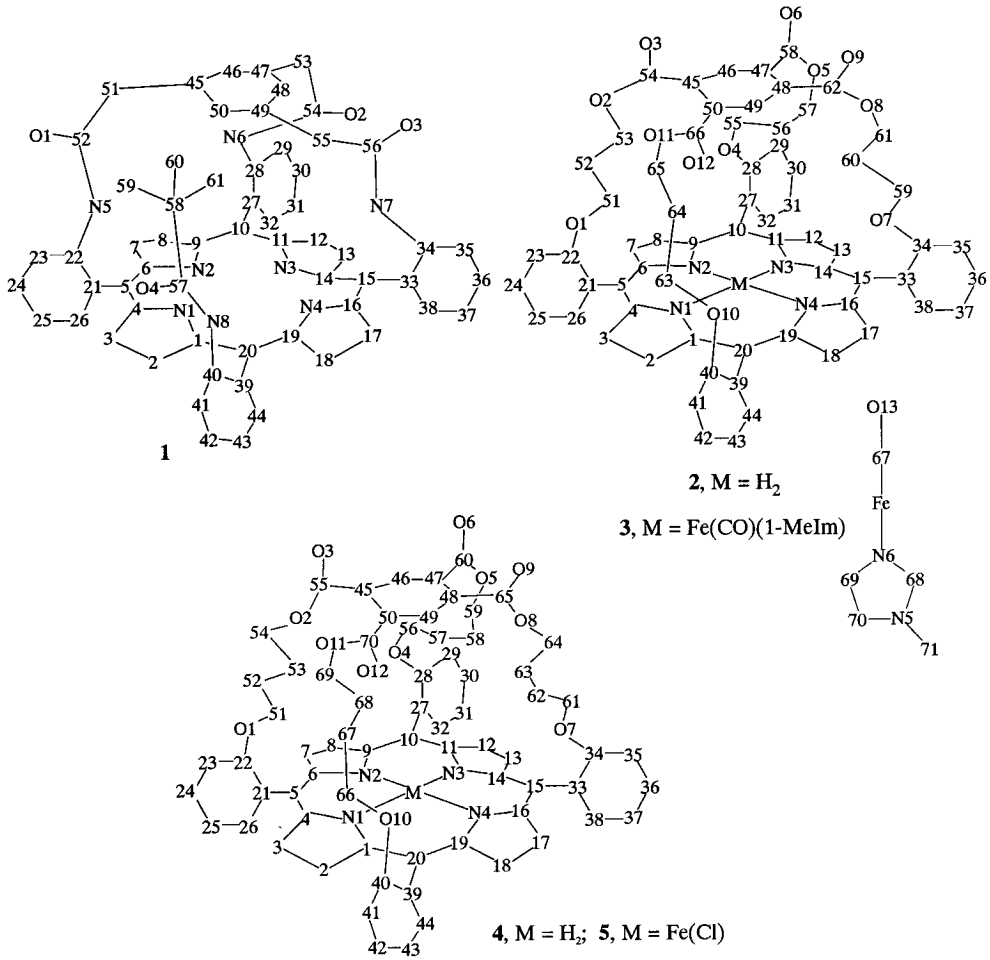

Figure 1. Labeling schemes for H_2-(α-PocPivP) (**1**), H_2(C_3-Cap) (**2**), Fe(C_3-Cap)(CO)(1-MeIm) (**3**), H_2(C_4-Cap) (**4**), and Fe(C_4-Cap)(Cl) (**5**).

of several months to afford X-ray quality crystals.

A crystal was coated in oil and mounted in the cold stream of a Picker diffractometer.[56] Unit cell dimensions and systematic absences were consistent with the monoclinic space group C_{2h}^5-$P2_1/n$. Badly disordered solvent could not be modeled successfully during structure refinement. Consequently, the BYPASS[57] subroutine in the program package PLATON[58] was used. In this method, potential solvent regions in the crystal structure are identified from considerations of space filling. The contributions to the total structure factors of the observed contents in these regions are calculated by a discrete Fourier transform, and the results are incorporated into the structure factors for further least-squares refinement of the ordered part of the structure. The procedure is iterated to convergence. In the present instance, electron density totaling 830 e$^-$ was subtracted, corresponding to a total of sixteen solvent molecules ($CHCl_3$ = 58 e$^-$ and hexane = 50 e$^-$) or four solvents per porphyrin

(56) Huffman, J. C. Ph.D. Dissertation, Indiana University, 1974.

(57) van der Sluis, P.; Spek, A. L. *Acta Crystallogr., Sect. A: Found. Crystallogr.* **1990**, *46*, 194−201.

(58) Spek, A. L. *Acta Crystallogr., Sect. A: Found. Crystallogr.* **1990**, *46*, C34.

Table 2. Selected Bond Distances (Å) for Porphyrins **1**−**5**

					Fe(C_4-Cap)(Cl)	
	H_2(α-PocPivP) (**1**)	H_2(C_3-Cap) (**2**)	Fe(C_3-Cap)(CO)(1-MeIm) (**3**)	H_2(C_4-Cap) (**4**)	(**5A**)	(**5B**)
Fe−C(CO)	−	−	1.800(13)	−	−	−
C−O(FeCO)	−	−	1.107(13)	−	−	−
Fe−L_{ax}	−	−	2.046(10)	−	2.243(3)	2.226(3)
av Fe−N_{eq}	−	−	1.99(2)	−	2.073(23)	2.071(7)
av N−C_a	1.370(2)	1.376(12)	1.388(12)	1.383(7)	1.381(12)	1.378(14)
av C_a−C_b	1.442(3)	1.451(12)	1.436(8)	1.424(11)	1.424(6)	1.423(11)
av C_b−C_b	1.344(6)	1.376(20)	1.356(17)	1.330(7)	1.337(13)	1.345(9)
av C_a−C_m	1.396(7)	1.372(14)	1.383(13)	1.394(6)	1.414(24)	1.407(14)

Table 3. Selected Bond Angles (deg) for Porphyrins **3** and **5**

		Fe(C_4-Cap)(L)	
	Fe(C_3-Cap)(CO)(L) **3** (L_{ax} = 1-MeIm)	**5A** (L_{ax} = Cl)	**5B** (L_{ax} = Cl)
O(CO)−C(CO)−Fe	178.0(13)	−	−
C(CO)−Fe−N(1)	89.9(4)	−	−
C(CO)−Fe−N(2)	90.6(5)	−	−
C(CO)−Fe−N(3)	92.3(5)	−	−
C(CO)−Fe−N(4)	92.1(5)	−	−
C(CO)−Fe−L_{ax}	178.9(5)	−	−
N(1)−Fe−L_{ax}	90.9(4)	99.4(2)	99.7(2)
N(2)−Fe−L_{ax}	88.7(4)	104.1(2)	104.7(2)
N(3)−Fe−L_{ax}	86.9(4)	105.2(2)	103.6(2)
N(4)−Fe−L_{ax}	88.6(4)	102.2(2)	99.8(2)
N(1)−Fe−N(2)	89.1(4)	88.3(4)	88.0(3)
N(1)−Fe−N(3)	177.9(3)	155.4(3)	156.7(3)
N(1)−Fe−N(4)	90.2(4)	87.0(4)	87.8(4)
N(2)−Fe−N(3)	90.9(4)	86.7(3)	86.0(4)
N(2)−Fe−N(4)	177.2(4)	153.7(3)	155.5(3)
N(3)−Fe−N(4)	89.7(4)	86.9(3)	88.3(3)

molecule. Prior to applying the BYPASS option, the electron density difference map suggested the presence of atoms heavier than carbon, so the solvent combination was assigned as one $CHCl_3$ and three *n*-hexane molecules per porphyrin. The final refinement[53] on F^2 of 739 variables and 7288 observations converged to the *R* indices given in Table 1. The atom-labeling scheme is given in Figure 1. Selected bond distances are given in Table 2. Additional crystallographic data, atomic coordinates and equivalent isotropic displacement parameters, additional bond lengths and angles, anisotropic displacement parameters, and hydrogen-atom coordinates and isotropic displacement parameters are available in Tables SVI−SX.[55]

Fe(C_3-Cap)(CO)(1-MeIm)·$CHCl_3$·$2H_2O$. Under a CO atmosphere Fe(C_3-Cap)(Cl) (∼20 mg) was dissolved in $CHCl_3$ (5 mL) and stirred over 0.3 M aqueous $Na_2S_2O_4$ for 5 min. The aqueous layer was removed. The $CHCl_3$ layer was dried over Na_2SO_4, one drop of 1-MeIm was added, and the solution was transferred to several diffusion tubes. X-ray quality crystals were obtained by slow diffusion of *n*-hexane into the $CHCl_3$ solution.

A crystal was coated in oil and mounted in the cold stream of a Picker diffractometer.[56] Cell dimensions and systematic absences were consistent with the space group C_{2h}^5-$P2_1/c$. Successful refinement of this structure was plagued by residual electron density that could not be modeled in a totally satisfactory way. Two strong residual electron density peaks did not resemble expected solvent molecules. Owing to their locations (2.55 Å (O14−O15) and 3.05 Å (O15−O15′)) they were presumed to be oxygen atoms of water molecules. Water could have been introduced during the reduction of the Fe center with aqueous $Na_2S_2O_4$. An anisotropic model for all atoms was not successful, presumably owing to deficiencies in our modeling of the solvent; all but the two water oxygen atoms and seven atoms of the porphyrin were refined anisotropically. The final refinement[53] on F^2 of 830 variables and 8694 independent observations converged to the *R* indices given in Table 1. The atom-labeling scheme is given in Figure 1. Selected bond distances and angles are given in Tables 2 and 3. Additional crystallographic data, atomic coordinates and equivalent isotropic displacement parameters, additional bond lengths and angles, anisotropic displacement parameters, and hydrogen-atom coordinates and isotropic displacement parameters are available in Tables SXI−SXV.[55]

H_2(C_4-Cap)·$2CHCl_3$. X-ray quality crystals were grown by slow diffusion of CH_3OH into a $CHCl_3$ solution of H_2(C_4-Cap) (**4**).

A crystal was coated in oil and mounted in the cold stream of a Picker diffractometer.[56] Cell dimensions and systematic absences were consistent with the orthorhombic space group D_{2h}^{14}-*Pbca*. Successful refinement of the structure was plagued by the presence of a disordered $CHCl_3$ solvate molecule, which was modeled as occupying two conformations with occupancies that refined to 0.46(1) and 0.54(1). An anisotropic model for the lighter atoms was not successful, presumably owing to deficiencies in our modeling of the solvent molecule so only the Cl atoms were refined anisotropically. The final refinement[53] on F^2 of 435 variables and 7053 independent observations converged to the *R* indices given in Table 1. The atom-labeling scheme is given in Figure 1. Selected bond distances are given in Table 2. Additional crystallographic data, atomic coordinates, equivalent isotropic displacement parameters and occupancies for all atoms (including hydrogen atoms), additional bond lengths and angles, and anisotropic displacement parameters are available in Tables SXVI−SXIX.[55]

Fe(C_4-Cap)(Cl)·$^1/_2CHCl_3$·$^1/_2C_6H_{14}$. X-ray quality crystals were grown by slow diffusion of *n*-hexane into $CHCl_3$ solution of Fe(C_4-Cap)(Cl) (**5**).

A crystal was coated in oil and mounted in the cold stream of an Enraf Nonius CAD4 diffractometer. Unit cell dimensions and the lack of systematic absences were consistent with the triclinic system. From the agreement among Friedel pairs the centrosymmetric space group $P\bar{1}$ was assumed. One arm to the cap and a $CHCl_3$ solvate were disordered. These were modeled as occupying two conformations. The occupancies found were 0.46 and 0.54 and 0.70 and 0.30 for the arm and the $CHCl_3$, respectively. Even after this refinement, significant residual electron density peaks remained that could not be easily interpreted. Consequently, the subroutine BYPASS[57] of the program package PLATON[58] was used. A total of 71 e^- was subtracted from the structure factors, corresponding to approximately 1/4 *n*-hexane per porphyrin molecule. The final refinement on F^2 involved an anisotropic model for all non-hydrogen atoms, except O11 and O11A, C68 and C68A, and C69 and C69A of the disordered arm and the atoms of the disordered $CHCl_3$. This refinement[53] of 1632 variables and 21119 observations converged to the *R* indices given in Table 1. The atom-labeling scheme is given in Figure 1. Selected bond distances and angles are given in Tables 2 and 3, respectively. Additional crystallographic data, atomic coordinates, equivalent isotropic displacement parameters, and occupancies for all atoms (including hydrogens), additional bond lengths and angles, and anisotropic displacement parameters are available in Tables SXX−SXXIII.[55]

Results and Discussion

Structure of H_2(α-PocPivP)·$2.5C_6F_6$. The crystal structure of H_2(α-PocPivP)·$2.5C_6F_6$ consists of the packing of one crystallographically independent porphyrin molecule and 2.5 hexafluorobenzene solvent molecules in the cell. There are no unusual intermolecular interactions. In the H_2(α-PocPivP) (**1**) portion of the structure the protected area consists of a benzene cap linked at the 1,3,5-positions by three-atom arms of the type $-CH_2(C{=}O)NH-$ to the ortho positions of three phenyl groups

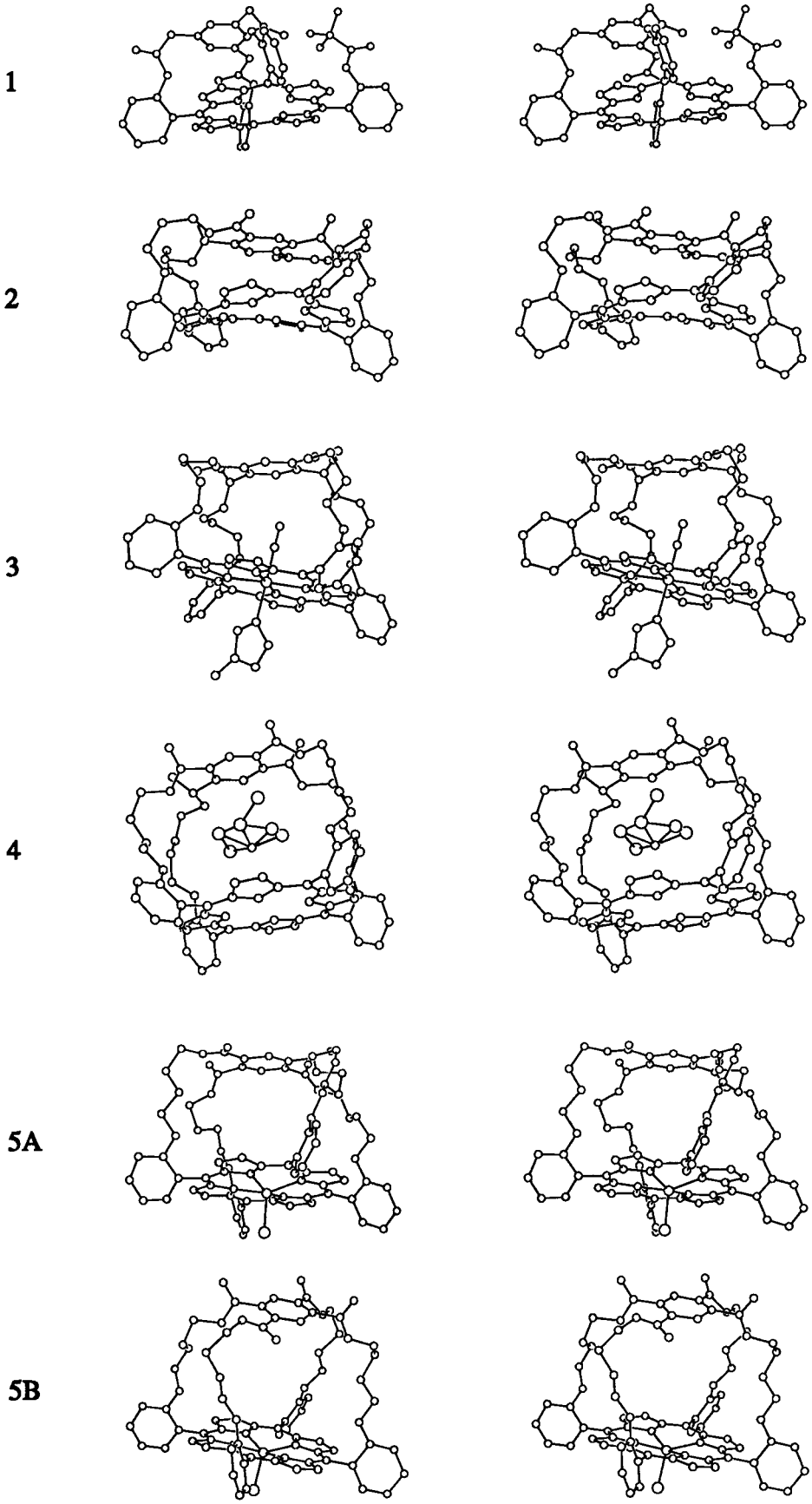

Figure 2. Stereoviews of **1**−**5**. Hydrogen atoms are omitted.

of 5,10,15,20-tetraphenylporphyrin. The pivalamido group, which is connected to the ortho position of the fourth phenyl group, extends in the α direction, or toward the cap. A stereoview of **1** is shown in Figure 2.

H_2(α-PocPivP)·2.5C_6F_6 is the fourth structure to be reported for the PocPivP system, but the first structure with no ligand under the cap. Its structure allows an analysis of the types and amounts of distortions that take place in the PocPivP system

Table 4. Porphyrin Distortions

structure	dihedral angle[a]	av deviation from 24-atom plane, Å	M deviation from 24-atom plane, Å[b]	vertical displacement of cap, Å[c]	lateral displacement of cap, Å[d]	∠Fe−C−O	ref
H_2(α-PocPivP)	12.7	0.10	−	4.21	1.86	−	this work
Ru(*β*-PocPivP)$(H_2O)_{in}(CO)_{out}$	13.7	0.21	0.20	4.23	3.01	178.3(3)	44
Ru(α-PocPivP)(CO)(1-MeIm)	9.9	0.13	−0.03	4.39	2.82	168(3)	43
	5.5	0.15	0.01	4.37	2.74	159(3)	
Fe(*β*-PocPivP)(CO)(1,2-Me_2Im)	17.6	0.27	0.01	4.25	3.30	172.5(6)	42
H_2(C_2-Cap)	0.0	0.13	−	3.96	0.12	−	45
Fe(C_2-Cap)(Cl)	3.2	0.08	0.47	4.01	0.24	−	47
Fe(C_2-Cap)(CO)(1-MeIm)	15.5	0.08	0.02	5.57	0.30	172.9(6)	46
	11.5	0.08	−0.01	5.67	0.00	175.9(6)	
H_2(C_3-Cap)	1.7	0.27	−	3.49	0.20	−	this work
Co(C_3-Cap)	1.9	0.31	0.06	3.50	0.20	−	48
Fe(C_3-Cap)(CO)(1-MeIm)	14.5	0.04	0.03	5.86	1.03	178.0(13)	this work
H_2(C_4-Cap)	6.0	0.08	−	7.28	0.69	−	this work
Fe(C_4-Cap)(Cl)	4.6	0.04	0.49	7.12	0.40	−	this work
	12.7	0.07	0.46	7.66	0.52	−	

[a] The dihedral angle is the interplanar angle between the cap and the 24-atom porphyrin plane. [b] Positive value indicates displacement toward the Cl or the CO group. [c] The vertical displacement of the cap is the perpendicular distance of the cap centroid from the mean 24-atom porphyrin plane. [d] The lateral displacement of the cap is defined as the distance of the cap centroid from the above perpendicular.

Table 5. Interplanar Angles (deg) and Amide Orientation for PocPivP Structures

compound	por-phenyl 1	por-phenyl 2	por-phenyl 3	por-phenyl 4	orientation of amide carbonyls 1 and 3
H_2(α-PocPivP)	72.1 (+)[a]	83.6	96.7 (−)	90.0	+/−[b]
Ru(α-PocPivP)(CO)(1-MeIm)	100.5 (+)	91.4	92.5 (+)	72.4	+/+
	62.8 (+)	87.8	84.6 (+)	71.3	+/−
Ru(*β*-PocPivP)$(H_2O)_{in}(CO)_{out}$	71.8 (+)	85.6	69.1 (+)	114.8	+/−
Fe(*β*-PocPivP)(CO)(1,2-Me_2Im)	108.8 (+)	97.4	101.8 (+)	119.1	+/+

[a] A (+) indicates the tilt of the phenyl ring moves the cap toward phenyl group 2 and a (−) indicates it moves it away. [b] A (+) indicates the oxygen atom of the amide carbonyl group is pointed toward phenyl group 2 and a (−) indicates that it is pointed away.

upon ligand binding. Table 4 summarizes these distortions. The centroid of the benzene cap in compound **1** is laterally displaced from a position directly above the porphyrin centroid by 1.86 Å; the cap lies 4.21 Å above the mean 24-atom porphyrin plane. In the other reported structures of the PocPivP system, Ru(α-PocPivP)(CO)(1-MeIm),[43] Ru(*β*-PocPivP)$(H_2O)_{in}(CO)_{out}$,[44] and Fe(*β*-PocPivP)(CO)(1,2-Me_2Im),[42] there is significant lateral displacement of the cap to accommodate the small molecule, but there is little vertical expansion. The cap moves laterally between 1.0 and 1.5 Å, from 1.86 Å in H_2(α-PocPivP) to 2.8 Å in Ru(α-PocPivP)(CO)(1-MeIm) and to 3.3 Å in Fe(*β*-PocPivP)(CO)(1,2-Me_2Im). However, the maximum vertical expansion is only 0.18 Å, from 4.21 Å in H_2(α-PocPivP) to 4.39 Å in Ru(α-PocPivP)(CO)(1-MeIm). These results suggest that the flexibility of the three-atom arms is severely limited, as would be expected for the more rigid amide functional groups. Close analysis of the PocPivP structures reveals that the lateral movement of the cap takes place through two types of distortion. First, the cap can move laterally away from the porphyrin centroid and toward the middle arm (attached to phenyl group 2) of the cap by the tilting of phenyl groups 1 and 3. The cap can also move laterally by orienting the amide carbonyl groups of the first and third arm so that they also point toward the phenyl group 2. Both of these types of motion serve to move the cap laterally away from the porphyrin centroid and in the direction of phenyl group 2. Table 5 summarizes interplanar angles between the porphyrin ring and the phenyl groups as well as the orientation of the amide groups. In H_2(α-PocPivP) the lateral displacement of the cap is the smallest of the four structures. The amide carbonyl group of one of the outer arms is oriented toward phenyl group 2 and the other carbonyl group is directed toward phenyl group 4. The tilts of phenyl groups 1 and 3 are also mixed, with phenyl 1 tilted toward phenyl 2 at an angle of 17.9° while phenyl 3 is tilted toward phenyl 4 at an angle of 6.7°. In Fe(*β*-PocPivP)(CO)(1-2-Me_2Im), which shows the greatest lateral displacement of the PocPivP structures, the conditions for lateral displacement of the cap are maximized. Phenyl groups 1 and 3 are tilted toward phenyl group 2 at angles of 18.8° and 11.8° from the perpendicular, respectively, and both the amide carbonyl groups of the outer arms of the cap are oriented toward phenyl 2.

The nonplanarity of the porphyrin plane in **1** (0.10 Å) is only slightly less than that of Ru(α-PocPivP)(CO)(1-MeIm) (0.13 Å and 0.14 Å), but significantly less than that of Ru(*β*-PocPivP)$(H_2O)_{in}(CO)_{out}$ (0.21 Å) and of Fe(*β*-PocPivP)(CO)(1,2-Me_2Im) (0.27 Å). This suggests that ligand binding has little effect on distortion of the porphyrin plane, but the orientation of the pivalamido (α or *β*) arm greatly affects nonplanarity. In the PocPivP compounds the dihedral angle between cap and porphyrin shows no noticeable trend with ligand binding or orientation of the arm.

H_2(C_3-Cap)·$CHCl_3$·3C_6H_{14} and Fe(C_3-Cap)(CO)(1-MeIm)·$CHCl_3$·2H_2O. Stereoviews of the porphyrin parts of these two structures are presented in Figure 2. Both H_2(C_3-Cap) (**2**) and Fe(C_3-Cap)(CO)(1-MeIm) (**3**) consist of the packing of one crystallographically independent porphyrin molecule and solvate molecules. The solvate molecules in H_2(C_3-Cap)·$CHCl_3$·3C_6H_{14} are disordered and were difficult to model. There are no unusual porphyrin−solvent interactions. The solvent molecules in Fe(C_3-Cap)(CO)(1-MeIm)·$CHCl_3$·2H_2O include one ordered $CHCl_3$ molecule and two others, assigned as water molecules. Notable intermolecular distances are 2.55 Å (O14(H_2O)−O15(H_2O)) and 3.05 Å (O15−O15′), both within range for hydrogen bonding interactions. The C_3-Cap of **2** and **3** consists of a 1,2,4,5 substituted benzene cap connected by four six-atom linkages of the type −(C═O)O(CH_2)$_3$O− to the ortho positions of the phenyl rings of 5,10,15,20-tetraphenylporphyrin. Compound **2** is unmetalated, whereas compound **3** is a six-coordinate iron species with CO bound to the Fe inside the cap and 1-MeIm bound to Fe trans to the CO ligand.

Table 6. Interplanar Angles (deg) for C_n-Cap Porphyrin Structures

compound	por-phenyl 1	por-phenyl 2	por-phenyl 3	por-phenyl 4
$H_2(C_2\text{-Cap})$	76.6	62.2	107.9	119.7
$Fe(C_2\text{-Cap})(Cl)$	106.7	68.1	96.0	113.1
$Fe(C_2\text{-Cap})(CO)(1\text{-MeIm})$	102.7	82.4	83.2	112.5
	97.7	75.9	69.6	104.2
$H_2(C_3\text{-Cap})$	47.3	92.2	52.4	81.8
$Co(C_3\text{-Cap})$	52.5	80.6	132.3	86.8
$Fe(C_3\text{-Cap})(CO)(1\text{-MeIm})$	72.2	114.4	69.0	73.2
$H_2(C_4\text{-Cap})$	75.7	70.3	66.0	68.2
$Fe(C_4\text{-Cap})(Cl)$	94.0	109.4	88.8	106.3
	112.3	74.5	69.0	97.7

The only previously known structure of a C_3-Cap system was that of $Co(C_3\text{-Cap})$.[48] The conformation of the porphyrin and cap in **2** compares well with that of $Co(C_3\text{-Cap})$ with regard to dihedral angle between cap and porphyrin, mean atomic deviation from the 24-atom plane, and vertical and lateral displacement of the cap (Table 4). In these two structures, where there is no ligand under the cap, the cap is twisted causing two opposite phenyl groups of tetraphenylporphyrin to deviate from being perpendicular to the porphyrin plane. Phenyl groups 1 and 3 of both compound **2** and $Co(C_3\text{-Cap})$ deviate from the perpendicular by between 37.5° and 42.7°, whereas in **3**, where there is a ligand under the cap, the largest deviation is only 24.4° (phenyl 2) (Table 6). Modest tilting occurs in the five-atom linked C_2-Cap porphyrin system (phenyls 2 and 4), but the longer arms of the C_3-Cap allow for significantly more distortion. The tilting of the phenyl groups is very different from that in the PocPivP system, where they tilt to move the cap away during ligand binding. In addition, unlike the PocPivP system, lateral movement of the cap is minimized, presumably owing to the presence of a fourth arm holding the cap over the porphyrin. The maximum displacement of a cap centroid from a position above the porphyrin centroid is 1.03 Å, significantly less than the displacement in all four of the PocPivP structures (Table 4). However, this displacement of 1.03 Å is sufficient to move the cap so that only atom C45 is above the oxygen atom (O13) of the carbonyl group at a distance of 3.174 Å.

The untwisting of the cap, in combination with the reorientation of the arms, causes the cap to expand vertically 2.36 Å to accommodate CO, from 3.5 Å in both **2** and $Co(C_3\text{-Cap})$ to 5.86 Å above the mean porphyrin plane in **3**. The size of the cavity and the amount of expansion that takes place are greater than those reported for the C_2-Cap system, where the cap expands approximately 1.6 Å, from 3.96 or 4.01 Å in $H_2(C_2\text{-Cap})$[45] and $Fe(C_2\text{-Cap})(Cl)$,[47] respectively, to 5.57 and 5.67 Å for the two crystallographically independent molecules of $Fe(C_2\text{-Cap})(CO)(1\text{-MeIm})$.[46] Unlike many of the nonlinear Fe−C−O linkages reported for Mb and Hb,[10,12] the Fe−C−O angle in **3** is essentially linear (178.0(13)°). This angle is consistent with the Fe−C−O angles reported for other heme model complexes (Table 7).

$H_2(C_4\text{-Cap})\cdot 2CHCl_3$ and $Fe(C_4\text{-Cap})(Cl)\cdot{}^1/_2CHCl_3\cdot{}^1/_2C_6H_{14}$. Stereoviews of the porphyrin $H_2(C_4\text{-Cap})$ (**4**) of $H_2(C_4\text{-Cap})\cdot 2CHCl_3$ and the two crystallographically independent porphyrin molecules of $Fe(C_4\text{-Cap})(Cl)$ (**5A** and **5B**) of $Fe(C_4\text{-Cap})(Cl)\cdot{}^1/_2CHCl_3\cdot{}^1/_2C_6H_{14}$ are presented in Figure 2. The structure of $H_2(C_4\text{-Cap})\cdot 2CHCl_3$ consists of the packing of one crystallographically independent porphyrin molecule and two chloroform solvate molecules. The $CHCl_3$ molecule, located under the cap is disordered and was modeled as occupying two positions with occupancies of 0.455(11) and 0.545(11). The structure of $Fe(C_4\text{-Cap})(Cl)\cdot{}^1/_2CHCl_3\cdot{}^1/_2C_6H_{14}$ consists of the packing of two crystallographically independent porphyrin molecules (**5A** and **5B**), one chloroform solvate, and one *n*-hexane solvate. The one hexane in the unit cell is comprised of two half molecules located at inversion centers. The solvent molecules were assigned and modeled as described above.

The C_4-Cap porphyrin has a benzene cap that is connected at the 1,2,4,5 positions by four seven-atom linkages of the type $-(CO)O(CH_2)_4O-$ to the ortho positions of the phenyl rings of 5,10,15,20-tetraphenylporphyrin. The compound $Fe(C_4\text{-Cap})(Cl)\cdot{}^1/_2CHCl_3\cdot{}^1/_2C_6H_{14}$ is the iron(III) chloride. The chloro ligand is outside the cap. The coordination geometry about the Fe atom is similar to that in other five-coordinate high-spin systems of the type Fe(Por)(Cl) (Table 8). The porphyrins **4**, **5A**, and **5B** are all similar with respect to dihedral angle between cap and porphyrin, deviation from the mean plane, and vertical and lateral displacements of the cap (Table 4).

The twisting that is seen in the C_3-Cap system when no ligand is bound under the cap in not seen in these C_4-Cap structures. Instead, the cap is already vertically extended. The presence of solvent under the cap in **4** makes it clear that there is ample space to accommodate small molecules, such as CO and O_2, as well as larger molecules, such as $CHCl_3$ or smaller axial bases. The binding of an axial base under the cap is reported for both the C_3-Cap and C_4-Cap systems.[34,59] The distances of the cap centroid from the porphyrin plane are 7.276, 7.125, and 7.664 Å in **4**, **5A**, and **5B** respectively. These distances are significantly longer than those for the two capped porphyrin carbonyl structures $Fe(C_2\text{-Cap})(CO)(1\text{-MeIm})$ (∼5.6 Å)[46] and $Fe(C_3\text{-Cap})(CO)(1\text{-MeIm})$ (5.86 Å). This suggests that ligand binding in the C_4-Cap system involves displacement of solvent or base under the cap.

Structure-Binding Relationships in Model Porphyrins. Table 9 lists O_2 and CO binding constants for selected model and biological systems. As noted earlier,[2] care must be exercised in comparing such data. Nevertheless, it is convenient to discuss trends in these binding data within the framework of central and peripheral steric effects that are presumed to occur on the distal, as opposed to the proximal side, of the protein or trans to the axial base for the models.[60] Central steric effects include any interactions from directly above the porphyrin plane; peripheral steric effects refer to side-on interactions. Central steric effects should reduce CO affinity but have little effect on O_2 affinity as CO bonds in a linear fashion whereas O_2 bonds in a bent fashion. For the same reason peripheral steric effects should reduce O_2 binding but not CO binding. One would expect that as the length of the C_n chains in these model systems is decreased with concomitant increase in central steric effects CO binding should decrease. Indeed, of the models in Table 9, the trends in *M* values for all but the C_n-Cap systems indicate discrimination against CO binding as the length of the arms or straps is decreased. Although *M* values for the C_n-Cap systems cannot be calculated from the available data, the trend in the values for $P_{1/2}{}^{CO}$ is unexpected, with C_2-Cap ≅ C_3-Cap < C_4-Cap.[33,34] There are two possible explanations for this trend. As we noted above, for C_4-Cap the binding of CO or O_2 may involve a displacement reaction rather than a simple ligation reaction. It is clear from the structure of $H_2(C_4\text{-Cap})\cdot 2CHCl_3$ that solvents can and do get trapped under the cap. If such solvent molecules are noncoordinating, for example toluene or $CHCl_3$, then in ligand binding studies there would be little change in the spectra, but there could be major changes in the binding constants compared with other porphyrin systems. Alternatively, there is the possibility that in solution the cap in the C_4-Cap system may be twisted to an even greater extent

(59) Ellis, P. E., Jr.; Linard, J. E.; Szymanski, T.; Jones, R. D.; Budge, J. R.; Basolo, F. *J. Am. Chem. Soc.* **1980**, *102*, 1889−1896.
(60) Traylor, T. G.; Campbell, D.; Tsuchiya, S.; Mitchell, M.; Stynes, D. V. *J. Am. Chem. Soc.* **1980**, *102*, 5939−5941.

Table 7. Metric Data for Selected Carbonylated Metalloporphyrins

	Fe−N (av) (Å)	Fe−C(CO) (Å)	C−O (Å)	Fe−C−O (deg)	Fe−L (trans to CO) (Å)	ref
Fe(TPP)(Py)(CO)[41]	2.02(3)	1.77(2)	1.12(2)	179(2)	2.10(1)	7
Fe(Deut)(CO)(THF)[41]	1.98(3)	1.706(5)	1.144(5)	178.3(14)	2.127(4)	65
Fe(Piv_2C_6)(CO)(1-MeIm)[41]	1.981(3)	1.733(4)	1.149(5)	178.3(5)	2.045(2)	40
Fe(Piv_2C_8)(CO)(1-MeIm)[41]	1.991(4)	1.752(4)	1.149(6)	178.0(5)	2.039(3)	40
Fe(Piv_2C_{10})(CO)(1-MeIm)[41]	1.999(3)	1.728(6)	1.149(6)	180.0(0)[a]	2.062(5)	21
Fe(PocPivP)(CO)(1,2-MeIm)	1.973(8)	1.768(7)	1.148(7)	172.5(6)	2.079(5)	42
Fe(C_2-Cap)(CO)(1-MeIm)						46
molecule 1	1.990(7)	1.742(7)	1.161(8)	172.9(6)	2.043(6)	
molecule 2	1.988(13)	1.748(7)	1.158(8)	175.9(6)	2.041(5)	
Fe(C_3-Cap)(CO)(1-MeIm)	1.992(21)	1.800(13)	1.107(13)	178.0(13)	2.046(10)	this work

[a] By symmetry.

Table 8. Metrical Data for Selected Fe(Por)(Cl) Systems

compound	av Fe−N, Å	Fe−Cl, Å	av N−Fe−N, deg	av N−Fe−Cl, deg	Fe dev from N_4 plane	Fe dev from 24-atom plane	ref
Fe(TPP)(Cl)[a]	2.049(9)	2.192(12)	−	−	0.38	0.38	66
Fe(TPP)(Cl)[b]	2.070(9)	2.211(1)	86.8	103.6	0.49	0.57	67
Fe(Proto)(Cl)[41]	2.062(10)	2.218(6)	87.0	103.3	0.48	0.55	68
Fe($Ph_{5,5}$-BHP)(Cl)[41]	2.060(2)	2.207(2)	87.25(5)	102.6(5)	0.46	0.45	14
Fe(TTOMePP)(Cl)[41]	2.079	2.207(20)	86.2	106	0.53	0.58	69
Fe(Durene-4/4)(Cl)[41]	2.054	2.232(1)	86.8	103.6	0.49	0.64	18
Fe(C_2-Cap)(Cl)	2.063(3)	2.242(1)	87.2(4)	102.8	0.46	0.47	47
Fe(C_4-Cap)(Cl)	2.07(2)	2.243(3)	87.2(4)	103(1)	0.46	0.43	this work
	2.071(7)	2.226(3)	87.5(5)	102(1)	0.49	0.46	

[a] Tetragonal form. [b] Monoclinic form.

Table 9. O_2 and CO Binding to Fe^{II} Porphyrin Complexes and Hemoproteins[a]

	$P_{1/2}^{O_2}$(Torr)	$P_{1/2}^{CO}$(Torr)	$M = P_{1/2}^{O_2}/P_{1/2}^{CO}$	ref
Mb (elephant)[b]	0.62	9.5×10^{-2}	6.5	70
Mb (horse)[b]	0.70	1.8×10^{-2}	39	71
R-state systems				
HbA(R)[b]	0.22(α)[d],0.36(β)[d]	1.4×10^{-3} [d]	160(α),260(β)	28, 72−75
Fe(PocPivP)(1-MeIm)	0.36	1.5×10^{-3}	240	28
Fe(MedPivP)(1-MeIm)	0.36	6.5×10^{-4}	550	28
Fe(C_2-Cap)(1-MeIm)	23, 4.5[c]	5.4×10^{-3}	4300	33, 49
Fe(C_2-Cap)(1,5-DCIm)	−	7.5×10^{-3}	−	34
Fe(C_3-Cap)(1,5-DCIm)	54[c]	4.1×10^{-3}	−	33
Fe(C_4-Cap)(1,5-DCIm)	−	0.21	−	34
Fe(Piv_2C_6)(1-MeIm)	0.16[d]	1.1×10^{-2}	14	77
Fe(Piv_2C_7)(1-MeIm)	0.033[d]	2.8×10^{-4}	120	77
Fe(Piv_2C_8)(1-MeIm)	0.13[d]	1.2×10^{-4}	1100	77
Fe(Piv_2C_{10})(1-MeIm)	0.030[d]	4.4×10^{-6}	6800	77
Fe(Durene-4/4)(1-MeIm)	69	1.4×10^{-2}	5×10^3	17
Fe(Durene-4/4)(DCIm)	139	2.3×10^{-2}	6×10^3	17
Fe(Durene-5/5)(DCIm)	83	1.2×10^{-3}	7×10^4	17
Fe(Durene-7/7)(DCIm)	152	1.5×10^{-3}	9×10^4	17
T-state systems				
HbA(T)[b]	40(α),[d]140(β)[d]	0.3[d]	130(α),470(β)	28, 74−76
Fe(PocPivP)(1,2-Me_2Im)	12.6	6.7×10^{-2}	220	28
Fe(MedPivP)(1,2-Me_2Im)	12.4	2.6×10^{-2}	480	28
Fe(TalPivP)(1,2-Me_2Im)	4	1.1×10^{-3}	3500	28
Fe(C_2-Cap)(1,2-Me_2Im)	4000	0.2	2.0×10^4	33, 49
Fe(C_3-Cap)(1,2-Me_2Im)	880[e]	0.14	−	33
Fe(C_4-Cap)(1,2-Me_2Im)	−	4.1	−	34
Fe(Piv_2C_6)(1,2-Me_2Im)	3.9[d,f]	0.53[d,f]	7	40
Fe(Piv_2C_7)(1,2-Me_2Im)	0.95[d,f]	3.3×10^{-2} [d,f]	29	40
Fe(Piv_2C_8)(1,2-Me_2Im)	5.1[d,f]	3.1×10^{-2} [d,f]	160	40
Fe(Piv_2C_{10})(1,2-Me_2Im)	2.7[d,f]	2.5×10^{-3} [d,f]	1100	40
Fe(Durene-4/4)(1,2-Me_2Im)	2.45×10^3	0.66	4×10^3	17
Fe(Durene-5/5)(1,2-Me_2Im)	2.31×10^3	4.8×10^{-2}	6×10^4	17
Fe(Durene-7/7)(1,2-Me_2Im)	2.19×10^3	3×10^{-2}	9×10^4	17

[a] Measurements were made in toluene at 25 °C, unless otherwise noted. [b] H_2O, pH ∼ 7. [c] 0 °C. [d] 20 °C. [e] −63 °C. [f] Solubilities of 7.00×10^{-6} M/torr and 9.47×10^{-6} M/torr for O_2 and CO, respectively, were used to calculate $P_{1/2}^{O_2}$ or $P_{1/2}^{CO}$ from the equilibrium constants.[78]

than is the cap in the C_3-Cap system. As a result, more energy would be required to reorient the molecule during ligand binding and this would manifest itself in a higher value of $P_{1/2}$.[34] The evident discrimination of the C_n-Cap system against O_2 binding (Table 9) is likely a result of peripheral steric effects. Unlike the durene, pocket, and Piv_2C_n systems, in the C_n-Cap systems linkages to the cap extend from all meso positions of the porphyrin so that peripheral steric interactions occur readily. The C_3-Cap structures make it clear that the porphyrin can twist significantly as well as reorient the arms to reduce peripheral steric effects, while the C_2-Cap system does not have that flexibility.

Central interactions can bring about three types of structural changes in proteins and models: (1) increased porphyrin ruffling or doming, (2) greater expansion of the distal protective group, or (3) tilting or bending or both of the Fe−C−O linkage. With the exception of one of the two crystallographically independent molecules of Ru(α-PocPivP)(CO)(1-MeIm), structural data for the pocket and capped porphyrin systems are consistent with conclusions reached earlier on the Piv_2C_n systems.[40] The main types of distortion that occur in the porphyrin upon CO ligation are ruffling of the porphyrin ring and expansion of the distal cavity, but not significant tilting or bending of the Fe−C−O linkage, as reported in many protein crystal structures. In the C_2-Cap and C_3-Cap systems, porphyrin ruffling decreases upon CO ligation, but there is significant expansion of the cap, while the Fe−C−O bond remains essentially linear. In the PocPivP system both the mean deviation from planarity and the lateral displacement of the cap increase when a small molecule binds underneath the cap (Table 4). One of the crystallographically independent molecules of Ru(α-PocPivP)(CO)(1-MeIm) has a Fe−C−O bond angle of 159(3)°, similar to that reported recently in the structure of mutant Mb(CO),[9,61,62] but nearer 180° than reported in the original Mb structures.[10,12] Since the pocket, Piv_2C_n, and durene model systems do sterically discriminate against CO binding and closely parallel the discrimination seen in Mb and the R- and T-states of Hb, it seems very likely that there is not significant off-axis distortion of the CO group in biological systems. Recent spectroscopic studies also support this conclusion.[63,64] In fact, in one such study[64] the Fe−C−O bond in Mb was found to be oriented ≤7° from the heme normal.

Acknowledgment. This research was kindly supported by U.S. National Institutes of Health (Grant HL13157). We thank Profs. Jack E. Baldwin and James P. Collman for the gifts of the porphyrins, and Dr. Kimoon Kim for help with the crystallizations.

Supporting Information Available: Tables SI−SV, SVI−SX, and SXI−SXV give crystallographic data, atomic coordinates and equivalent isotropic displacement parameters, additional bond lengths and angles, anisotropic displacement parameters, and hydrogen atom coordinates and isotropic displacement parameters for **1**, **2**, and **3**, respectively. Tables SXVI−SXIX and SXX−SXXIII give crystallographic data, atomic coordinates, equivalent isotropic displacement parameters, and occupancies for all atoms (including hydrogens), additional bond lengths and angles, and anisotropic displacement parameters for **4** and **5**, respectively (61 pages). This material is contained in many libraries on microfiche, immediately follows this article in the microfilm version of the journal, can be ordered from ACS, and can be downloaded from the Internet; see any current masthead page for ordering information and Internet access instructions.

JA953684X

(61) Springer, B. A.; Sligar, S. G.; Olson, J. S.; Phillips, J., George, N. *Chem. Rev.* **1994**, *94*, 699−714.
(62) Cameron, A. D.; Smerdon, S. J.; Wilkinson, A. J.; Habash, J.; Helliwell, J. R.; Li, T.; Olson, J. S. *Biochemistry* **1993**, *32*, 13061−13070.
(63) Ray, G. B.; Li, X.-Y.; Ibers, J. A.; Sessler, J. L.; Spiro, T. G. *J. Am. Chem. Soc.* **1994**, *116*, 162−176.
(64) Lim, M.; Jackson, T. A.; Anfinrud, P. A. *Science* **1995**, *269*, 962−966.
(65) Scheidt, W. R.; Haller, K. J.; Fons, M.; Mashiko, T.; Reed, C. A. *Biochemistry* **1981**, *20*, 3653−3657.
(66) Hoard, J. L.; Cohen, G. H.; Glick, M. D. *J. Am. Chem. Soc.* **1967**, *89*, 1992−1996.
(67) Scheidt, W. R.; Finnegan, M. G. *Acta Crystallogr., Sect. C: Cryst. Struct. Commun.* **1989**, *45*, 1214−1216.
(68) Koenig, D. F. *Acta Crystallogr.* **1965**, *18*, 663−673.
(69) Ji, L. N.; Liu, M.; Huang, S. H.; Hu, G. Z.; Zhou, Z. Y.; Koh, L. L.; Hsieh, A. K. *Inorg. Chim. Acta* **1990**, *174*, 21−25.
(70) Romero-Herrera, A. E.; Goodman, M.; Dene, H.; Bartnicki, D. E.; Mizukami, H. *J. Mol. Evol.* **1981**, *17*, 140−147.
(71) Antonini, E.; Brunori, M. *Hemoglobin and Myoglobin in Their Reactions with Ligands*; Frontiers of Biology 21; North-Holland Publishing: Amsterdam, 1971.
(72) Gibson, Q. H. *J. Biol. Chem.* **1970**, *245*, 3285−3288.
(73) Olson, J. S.; Anderson, M. E.; Gibson, Q. H. *J. Biol. Chem.* **1971**, *246*, 5919−5923.
(74) Sharma, V. S.; Schmidt, M. R.; Ranney, H. M. *J. Biol. Chem.* **1976**, *251*, 4267−4272.
(75) Steinmeier, R. C.; Parkhurst, L. J. *Biochemistry* **1975**, *14*, 1564−1572.
(76) Sawicki, C. A.; Gibson, Q. H. *J. Biol. Chem.* **1977**, *252*, 7538−7547.
(77) Momenteau, M.; Loock, B.; Tetreau, C.; Lavalette, D.; Croisy, A.; Schaeffer, C.; Huel, C.; Lhoste, J.-M. *J. Chem. Soc., Perkin Trans. 2* **1987**, 249−257.
(78) Lavalette, D.; Tetreau, C.; Mispelter, J.; Momenteau, M.; Lhoste, J.-M. *Eur. J. Biochem.* **1984**, *145*, 555−565.